Optical Switching and Networking 21 (2016) 67–78

Contents lists available at ScienceDirect

Optical Switching and Networking

journal homepage: www.elsevier.com/locate/osn

Delay and estimation uncertainty in distributed power control algorithm for optical CDMA networks

Fábio Renan Durand [a], Bruno Augusto Angélico [b], Taufik Abrão [c,*]

[a] Universidade Tecnológica Federal do Paraná (UTFPR), Cornélio Procópio, Brazil
[b] Depto. de Engenharia de Telecomunicações e Controle (PTC), Escola Politécnica da Universidade de São Paulo (EPUSP), Brazil
[c] Department of Electrical Engineering, State University of Londrina (DEEL-UEL), Brazil

ARTICLE INFO

Article history:
Received 16 August 2015
Received in revised form
30 January 2016
Accepted 22 February 2016
Available online 2 March 2016

Keywords:
Distributed power control algorithm
Time-delay
Estimation uncertainty
Optical CDMA networks

ABSTRACT

In this work, the performance of a distributed power control algorithm (DPCA) considering time-delay and estimation uncertainty has been investigated. Control theory concepts have been deployed aiming to derive the Foschini–Miljanic DPCA as well as to analyse their stability properties under time-varying delays and estimation uncertainty applicable to optical networks. Although delays introduce transient response for initial iterations, our numerical results have shown a suitable convergence of the transmitted power obtained with the DPCA under strong delay conditions. Furthermore, the DPCA was able to converge also under high level of uncertainty on the estimated SNIR, despite the solution quality decreasing.

1. Introduction

The code division multiple access (CDMA) is considered an alternative method of access in optical and wireless networks [1]. In this type of access, each user is recognised by its code and different codes can share a given common channel. In the common channel, the interference that may arise between different codes is known as the multiple access interference (MAI) and can limit the number of users utilising the channel simultaneously [2]. The advantages of the CDMA are asynchronous transmission, soft capacity on demand, high degree of scalability, communication security, non-existence of packet collisions and quality of service (QoS) at the physical layer [1,2].

In the CDMA-based networks, distinct distances between the nodes introduce the near-far problem, thus an efficient power control is needed to overcome this problem and enhance the performance and the throughput of the network [3,4]. In this case, the distributed power control (DPC) is one of the most important issues in resource allocation and system optimisation because of its significant impact on both performance and capacity [3]. The distributed power control algorithm (DPCA) is an effective way to avoid the near-far problem and to increase the optical system capacity [4,5]. In addition, recent researches have demonstrated the utilisation of resource allocation strategies and optimisation algorithms, such as local search, simulated annealing, genetic algorithm, particle swarm optimisation, ant colony optimisation (ACO), as well as game theory results, aiming to regulate the transmitted power, bit rate variation, and number of active users in order to maximize the aggregate throughput of the optical networks [6–9].

However, the complexity and fairness of such strategies represent aspects to be improved. In this context, the analytical DPCA, proposed by Foschini and Miljanic (FM), which utilises a linear update scheme and is able to

* Corresponding author.
E-mail addresses: fabiodurand@utfpr.edu.br (F.R. Durand), angelico@lac.usp.br (B.A. Angélico), taufik@uel.br (T. Abrão).

http://dx.doi.org/10.1016/j.osn.2016.02.002
1573-4277/

converge to specific signal-to-noise plus interference ratio (SNIR) requirement, is still quite attractive [4,10]. The analytical-iterative characteristic of the analytical DPCAs makes them attractive due their performance-complexity tradeoff regarding the optimisation methods that use numerical approaches, heuristics and matrix inversion [6–9]. The impact of FM-DPCA on the global system performance can be seen as the increase on the throughput and simultaneously the decrease on the packet delay with only a few iterations of the DPCA. For instance, it is necessary that approximately 7% of the total number of iterations deployed by the FM-DPCA to achieve convergence at a point where the throughput and delay achieve the value close to the optimum one [4]. Another analytical DPCA proposed is based on the Verhulst model, which tries to describe the temporal evolution of the number of individuals of some biological species [11,12].

In real communication systems, DPCAs require communication among the nodes. However, processing time including coding and decoding, propagation delay and waiting of availability of channels for transmission all introduce delays into the network. Delays, which can be heterogeneous and time varying are inevitably present in the communication system, and definitively affect the interference level measurements in such algorithms [13]. Hence, these aspects cannot be neglected in realistic models since it is well-known that they can potentially lead to instabilities and oscillatory behaviour [14]. In this context, this work proposes and analyses for the first time, as far as the authors are aware, the performance of a DPCA based on Foschini and Miljanic (FM) power control model considering both practical issues, the time-delay and estimation uncertainty in optical CDMA networks. These networks bring a new combination of challenges with the power control, such as links greater than wireless networks, and self generation of the optical amplified spontaneous emission (ASE) noise in the preamplifier, as well as the MAI generated by the optical codes [3]. In [15], the effect of time-delay on the FM-based power control has been considered for a wireless CDMA network.

In optical networks, the signal propagation delay cannot be ignored, because there is a round-trip propagation bigger than the propagation delay of wireless CDMA-based networks. If the processing time (including coding, decoding and the waiting for channel availability) is considered in addition to the signal propagation delay, the time delay can be tens of milliseconds. Moreover, the stability cannot be guaranteed, given a sufficiently large time-delay and an algorithmic update period similar to the duration of the time-delay.

We have deployed some aspects from the control theory perspective in order to derive results for the FM-DPCA algorithm aiming to demonstrate that stability properties are maintained in the presence of time-varying delays. The advantage of using a control theory framework is that stability and estimation uncertainty can be jointly studied [16].

1.1. Related works

The importance of investigating specific techniques for systems with delay is prompted by the fact that the existence of a delay might cause instabilities [14]. These characteristics were analysed considering a FM-based DPCA algorithm for wireless network, where the algorithm was shown to remain stable in the presence of constant propagation delays [17]. However, channel characteristics change with time, so delays in communications networks are time-varying by nature. This kind of delays was studied in [18], which proved the stability for constant arbitrarily large delays. However, in practice, it is not possible to ensure a constant delay, so the model must include the effect of the possible variability of the time delays. The stability of the FM algorithm in the presence of the inherent time-varying was characterised with positive systems theory [19]. In [20] it was proved that if a feasible steady power allocation exists, this will be asymptotically stable for arbitrary gains and heterogeneous, time varying delays. In the analysis it was made use of Lyapunov Razumikhin functions to address the infinite dimensional character of the problem, with delay independence being a result of certain contraction properties of the interference from other users. In [21] the current theory on positive systems was extended in order to account for positive systems with time-varying delays. The results showed that FM algorithm is unconditionally stable (convergent) even in presence of bounded time-varying communication delays, and in presence of topology changes. In [15] the effects of time-varying delays and uncertainty in the measurement of the SINR for FM in wireless networks were investigated. The stability analyses utilise a graphical methodology based on the small gain theorem and have shown the precision and robustness of the FM algorithm. In [13], the problem of distributed power control in wireless network was studied from a control theory perspective. It was showed the importance of transmission delays with respect to stability and performance. In [16], an unified framework to design and analyse uplink distributed power control schemes from a control theory perspective for CDMA cellular system was proposed. The effects of linear detectors and round trip delays are explicitly characterised in this study. Under this perspective, the FM scheme provides a simple distributed control law that can be tuned to tolerate delays in the feedback systems, but at the expense of affecting the transient tracking properties for the objective SINR. In [4] the FM-DPCA has been extended to optical networks operation when physical restrictions should be considered; numerical results have shown that the introduction of some level of power control in the random access OCDMA networks demonstrates be very profitable to the throughput increasing.

In this realistic context, the network performance optimisation facing constraints, such as communication delay and signal transmission power management is challenging, especially in optical CDMA networks under realistic scenarios where the propagation delay and the estimation uncertainty constitute salient issues. The estimation uncertainty of the optical channel depends on the several factors such as monitoring approach, physical impairments and the dynamic of the adopted resource allocation policy [22].

1.2. Contribution and organization

The main contributions of the work are twofold: (a) description of a distributed power control algorithm based on the Foschini–Miljanic model suitable for optical CDMA under the perspective of control theory; (b) stability analysis based on control theory in order to derive results for the FM-DPCA algorithm under time-varying delays and estimation uncertainty.

The rest of the paper is organised in the following manner: Section 2 presents the adopted optical network topology system model and the associated power control problem. Stability analysis of the derived DPCA under delay conditions and estimation uncertainty is developed in Section 3. Some aspects regarding the computational complexity and packet delay performance are shown in Section 4. in Afterward, numerical results are discussed in Section 5 for access optical networks operation scenarios. Main conclusions are offered in Section 6.

2. System model

2.1. Network architecture

The optical CDMA network architecture is based on a broadcast-and-select pattern formed by K nodes interconnected by passive star coupler. For viability characteristics, it was considered that network equipment, such as code-processing devices (encoders and decoders at the transmitter and receiver) and star coupler could be made using robust, lightweight, and low-cost platforms with commercial-off-the-shelf technologies [1].

The transmitting and receiving nodes create virtual path, based on the code, and the total link length is given by $d_{ij} = d_i^{tx} + d_j^{rx}$, where d_i^{tx} is the link length from the ith transmitting node to the star coupler and d_j^{rx} is the link length from the jth receiving node to the star coupler. The received power at a jth node is given by $P_R = a_{Star} P_i \exp(-a \cdot d_{ij})$ and $a_{Star} = 10\log_{10}K - (\log_2 K)10\log_{10}\delta$, where P_i is the transmitted power by ith transmitting node, a is the fiber attenuation, a_{Star} is the star coupler attenuation and δ is the excess loss relation [3]. Although, there are a lot of encoding methods for 2D codes, we have adopted the carrier-hopping prime codes (CHPCs) considering their characteristics of the low complexity of code construction, the flexibility of the wavelength and code length chosen and the correlation property [2]. The CHPC code could be obtained by array waveguide gratings (AWG) encoder/decoder that essentially creates a combination of two patterns: a wavelength-hopping pattern and a time-spreading pattern [2,23]. The AWG encoder/decoder has approximately uniform loss of 6 dB independently of the number of wavelengths (N_λ) [23].

The 2D codes are a key concept in order to implement the time-wavelength coded (2D) optical CDMA networks. They can be represented by $N_\lambda \times N_T$ matrices, where N_λ is the number of rows, that is equal to the number of available wavelengths, and N_T is the number of columns, that is equal to the code length. The code length is determined by the bit period T_B, which is subdivided in small units called chips, each of duration $T_c = T_B/N_T$. In each code there are w short pulses of different wavelength, where w is called the weight of the code. An $(N_\lambda \times N_T, w, \lambda_a, \lambda_c)$ code is the collection of binary $N_\lambda \times N_T$ matrices each of code weight w, being λ_a and λ_c non-negative integers representing the constraints on the autocorrelation and cross-correlation [2].

2.2. Power control mechanism

The power control in optical networks is an optimisation problem. Denoting Γ_i as the carrier to interference ratio (CIR) at the required decoder input, in order to get a certain maximum bit error rate (BER) tolerated by the ith optical node, and defining the K-dimensional column vector of the transmitted optical power $\mathbf{p} = [p_1, p_2, \ldots, p_K]^\top$, then the optical power control problem consists of finding the (optimal) optical power vector $\mathbf{p}$ that minimises the cost function [3] $J(\mathbf{p})$, subject to the constraints Γ_i and $[P_{\min}; P_{\max}]$, formally:

$$\begin{aligned}
&\text{minimize} \quad J(\mathbf{p}) = \mathbf{1}^T\mathbf{p} = \sum_{i=1}^{K} p_i \\
&\text{subject to:} \quad \Gamma_i = \frac{G_{ii} p_i[n]}{\sum_{j=1, j\neq i}^{K} G_{ij} p_j[n] + \sigma_i^2} \geq \Gamma_i^*, \\
&P_{\min} \leq p_i \leq P_{\max}, \quad \forall i = 1, 2, \ldots, K,
\end{aligned} \tag{1}$$

where $\mathbf{1}^\top = [1, \ldots, 1]$ and Γ_i^* is the minimum CIR to achieve a desired quality of service (QoS), G_{ii} is the attenuation of the user considering the power loss between the nodes according network topology, G_{ij} corresponds to the attenuation factor for the signal of interfering user j, σ_i^2 is the noise power, p_i is the transmitted power for i-node, and p_j is the transmitted power for interfering nodes.

In terms of signal-to-noise plus interference ratio (SNIR), Eq. (1) can be written as

$$\begin{aligned}
&\gamma_i = \frac{N_T^2 G_{ii} p_i[n]}{\rho^2 \sum_{j=1, j\neq i}^{K} G_{ij} p_j[n] + \sigma_i^2} \geq \gamma_i^* \\
&P_{\min} \leq p_i \leq P_{\max}, \quad \forall i = 1, 2, \ldots, K,
\end{aligned} \tag{2}$$

where ρ is the average variance of the Hamming aperiodic cross-correlation amplitude and N_T is code length. Using matrix notations, (2) can be written as

$$[\mathbf{I} - \mathrm{diag}(\boldsymbol{\gamma}^*)\mathbf{H}]\mathbf{p} \geq \mathbf{g} \tag{3}$$

where $\mathbf{I}$ is an identity matrix, $\mathbf{H}$ is the normalised interference matrix, whose elements can be evaluated by $H_{ij} = (\rho^2 G_{ij})/(N_T^2 G_{ii})$, for $i \neq j$, and zero otherwise. The term $g_i = (\gamma_i^* \sigma_i^2)/(N_T^2 G_{ii})$ represents a scaled version of the noise power [4]. The notation $\mathrm{diag}(\boldsymbol{\gamma}^*)$ represents a diagonal matrix whose diagonal elements are the components of vector $\boldsymbol{\gamma}^* = [\gamma_1^* \gamma_2^* \cdots \gamma_K^*]^\top$.

Substituting inequality by equality, it is possible to obtain the power vector solution through matrix inversion $\mathbf{p}^* = [\mathbf{I} - \mathrm{diag}(\boldsymbol{\gamma}^*)\mathbf{H}]^{-1}\mathbf{g}$. The matrix inversion is equivalent to a centralised power control, i.e., the existence of a central node to power control. The central node stores information about all physical network architecture, like link length between nodes, regular update about link establishment and dynamic of traffic [5]. These observations justify the need for on-line SNIR optimisation algorithms, which have provable convergence properties for general network configurations [10,12].

The DPCA synthesis consists of developing a systematic procedure for the evolution of the vector $\mathbf{p}$ in order to reach the optimum value $\mathbf{p}^*$, based on the target SNIR, γ_i^*, on γ_i and p_i values. For dealing with DPCA, it is more convenient to rewrite Eq. (2) as [16]:

$$\gamma = \begin{bmatrix} \gamma_1[n] \\ \vdots \\ \gamma_K[n] \end{bmatrix} = f(\mathbf{p}[n], \mathbf{y}[n]) \triangleq \begin{bmatrix} p_1[n]/y_1[n] \\ \vdots \\ p_K[n]/y_K[n] \end{bmatrix} \tag{4}$$

where,

$$\mathbf{y}[n] = \mathbf{H}\mathbf{p}[n] + \varsigma \tag{5}$$

with ς the vector with components $\varsigma_i = (\sigma_i^2)/\left(N_T^2 G_{ii}\right)$.

The FM-DPCA algorithm solution for the power allocation problem satisfies the following associate iterative process [10]:

$$p_i[n+1] = p_i[n] - \alpha\left(1 - \frac{\gamma_i^*}{\gamma_i[n]}\right)p_i[n], \quad i = 1, \ldots, K, \tag{6}$$

where n is the number of iterations and α is the numerical integration step that converges for $0 < \alpha < 1$. Indeed, Eq. (6) represents the classical DPCA proposed by Foschini and Miljanic for CDMA wireless network [10] and it can be effectively adapted for each optical node in an optical network. Indeed, the FM-DPCA can be implemented in each optical node because all necessary parameters (γ_i^* and $p_i[n]$) are known at each single node. Thus, (6) depends on local parameters, allowing the power control to work in a distributed manner.

The quality of the solution (after convergence) can be analysed in terms of normalised mean squared error (NMSE) related to p^*, calculated as:

$$\mathrm{NMSE}[n] = \mathbb{E}\left[\frac{\| \mathbf{p}[n] - \mathbf{p}^* \|^2}{\| \mathbf{p}^* \|^2}\right], \tag{7}$$

where $\|\cdot\|^2$ denotes the square Euclidian distance to the origin, and $\mathbb{E}[\cdot]$ the expectation operator. Hence, the quality of solution is measured by how close to the optimum solution is $p[n]$ at nth iteration.

3. Stability analysis

In this section, the distributed closed-loop linear power control is analyzed in terms of control theory, by considering an independent control law per user [13]. In this formulation, it is assumed that the receiving node estimates the SINR and calculates the error in the regulation of this variable. This information is sent to the transmitting node, which next adjusts its power level assisted by DPCA. This feedback loop is illustrated in Fig. 1.

The time delay represents the sum of forward propagation delay of a signal from its transmitting node to receiving node and feedback propagation delay of a signal from the SNIR output at receiving node to the transmitting node. The control problem can be formulated by designing a power assignment law such that the measured SINR, $\gamma_i[n]$, reaches its reference SINR, γ_i^*, in steady state. In this sense, discrete version of the FM model, Eq. (6) can be written as:

$$\begin{aligned} p_i[n+1] &= p_i[n] + \alpha\left(1 - \frac{\gamma_i^*}{\gamma_i[n]}\right)p_i[n], \\ &= p_i[n] + u[n] \quad i = 1, \ldots, K \end{aligned} \tag{8}$$

Fig. 2 presents the equivalent closed loop system in vectorial form, where $\mathbf{u}[n]$ represents the power update and $\mathbf{C}(\cdot)$ the controller. It is also assumed that n_f and n_b represent the forward and backward delays in the feedback system, respectively.

From the first line of (8), it is possible define the following error function at nth instant for the ith receiver:

$$\epsilon_i[n] = \left\{1 - \frac{\gamma_i^*}{\gamma_i[n]}\right\}p_i[n] = p_i[n] - \hat{p}_i[n]. \tag{9}$$

being $\hat{p}_i[n] = \frac{\gamma_i^*}{\gamma_i[n]}p_i[n]$ the time-varying power references. Note that the reference for the ith node in (9) depends on the transmission power of the remaining active nodes. Consequently, if a distributed power control perspective is followed, where each transmitter updates its transmission power based on its own error measurement in (9), then linear feedback systems are obtained after this transformation for each user. In practice, there are transport delays in the forward and backward transmissions as well [16], as shown in Fig. 2. The sources of these delays could be from the SINR estimation procedure in the receiving node, processing time (coding and decoding), propagation delay and waiting of channel availability for transmission [14,16–21,15]. Hence, (9) can be redefined accordingly as:

$$\epsilon_i[n] = p_i[n - n_b] - \hat{p}_i[n - n_b], \tag{10}$$

which in the z-domain is given by:

$$\epsilon_i(z) = z^{-n_b}\{p_i(z) - \hat{p}_i(z)\}. \tag{11}$$

Defining

$$a_i(z) = z^{-n_b} e_i(z), \tag{12}$$

as shown in Fig. 2. Therefore, the power assignment rule

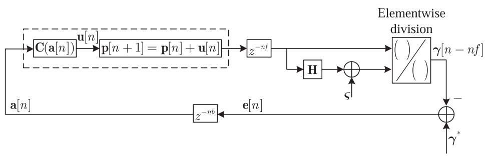

Fig. 2. Feedback diagrams for power control.

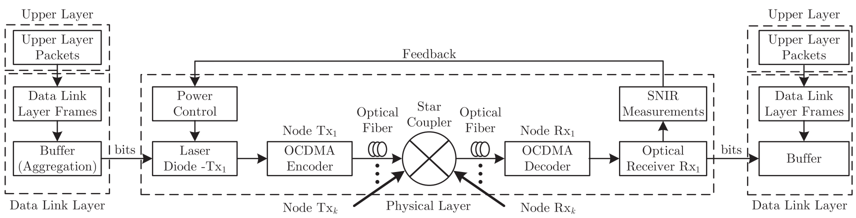

Fig. 1. Closed-loop power assignment in optical CDMA network.

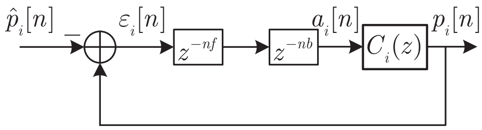

Fig. 3. Equivalent feedback diagrams for power control.

given by DPCA based on FM algorithm is represented as

$$p_i[n+1] = p_i[n] + \alpha a_i[n] \tag{13}$$

The distributed control transfer function is then written as

$$C_i(z) = \frac{p_i(z)}{a_i(z)} = \frac{\alpha z^{-1}}{1 - z^{-1}} \tag{14}$$

The equivalent feedback diagram is depicted in Fig. 3.

It is possible to see that the close loop transfer functions are given by

$$T_i(z) = \frac{p_i(z)}{\hat{p}_i(z)} = \frac{-C_i(z) z^{-(n_f+n_b)}}{1 + C_i(z) z^{-(n_f+n_b)}} \tag{15}$$

Substituting (14) in (15), it follows that

$$T_i(z) = \frac{-\alpha z^{-(1+n_{n_f}+n_{n_b})}}{1 - z^{-1} + \alpha z^{-(1+n_{n_f}+n_{n_b})}} \tag{16}$$

Hence, the condition for stability is that the roots of $z^{(1+n_{n_f}+n_{n_b})} - z^{(n_{n_f}+n_{n_b})} + \alpha$ must lie into the unit circle. In [13] it is shown that, for the system to be stable, α must satisfy the following limits:

$$0 < \alpha < \sqrt{2\left[1 - \cos\left(\frac{\pi}{2(n_f+n_b)+1}\right)\right]}. \tag{17}$$

The SNIR at the receiving node is not perfectly estimated and the values obtained from these estimations present a stochastic error attribute. In order to incorporate this characteristic, a random uncertainty is added to the calculated SNIR at each iteration. The uncertainty of the estimated SNIR is given by ζ, where ζ will be considered as a random variable with an uniform distribution within $\zeta \sim \mathcal{U}[-\delta; +\delta]$. Hence, the estimated SNIR at each iteration is given by:

$$\hat{\gamma}_i = (1+\zeta)\gamma_i, \quad \forall i \quad \text{and} \quad \zeta \in [-\delta; +\delta]. \tag{18}$$

4. Computational complexity and packet delay performance

The tradeoff between the FM-DPCA performance and the computational time considering the delay is evaluated in two aspects. The computational complexity of the algorithm and packet delay performance have been analysed. The computational complexity usually refers to the upper bound for the asymptotic computational complexity, which quantifies the amount of time taken by an algorithm to run as a function of their input size. In the FM-DPCA algorithm, the computational complexity depends on the number of sum and multiplication operations. Thus, the computational complexity of the FM-DPCA with and without delay is of the order $\mathcal{O}(K^2)$, where K is the number of nodes. In this case, the delay will not affect the complexity since it does not increase the number of the operation in the FM-DPCA. This computational complexity is obtained in the same way of [24]. For comparison purpose, the computational complexity required for matrix inversion considering the best situation is given by $\mathcal{O}(K^2 \cdot \log K)$ [25].

On the other hand, although in the OCDMA various codes could be transmitted simultaneously, the increase of the MAI can limit the network performance. In this sense, it is necessary to consider coordinated access schemes, random access protocols or medium access control (MAC) that prevents the throughput degradation, variable-transmission-rate, as well as different QoS metrics for different users [4–6]. The slotted ALOHA (or S-ALOHA) is a better protocol when the user's activity and the offered traffic are high, whereas the other one, like round robin receiver/transmitter (R^3T) procedure is better for smaller values of user activity and moderate traffic [4]. However, the R^3T higher performance is achieved at the expense of higher delay and system complexity. The packet delay performance considering the S-ALOHA integrated with FM-DPCA is utilized to evaluate the effects of the system delay, that is related to the propagation delay in this work. The packet delay represents the time duration from its generation to the moment it is successfully transmitted. The average packet delay is given by [4,5],

$$D = \frac{\overline{n}}{\beta} + 1 \tag{19}$$

where $\overline{n}$ and β are the expected channel backlog and the steady-state throughput, respectively. In a backlog condition, an attempt to transmit a new packet fails and the node cannot generate new packets until the backlogged packet is received correctly. The throughput represents the expected number of successful packets per slot, however when the system delay is considered the time slot became $1+b$, where $b = \tau/T$ is the normalized delay for end-to-end delay (τ) and packet transmission time (T). On other hand, $b=0$ for no system delay. Moreover, the arrival distribution can be approximated by a binomial distribution; hence, the steady-state throughput will be given by [4]

$$\beta = \sum_{i=1}^{K} i \cdot \binom{K}{i} \left(\frac{\overline{G}}{K}\right)^i \left(1 - \frac{\overline{G}}{K}\right)^{K-i} \cdot P_C(i) \tag{20}$$

where $\overline{G}$ is the average offered traffic rate. The average offered traffic is composed of newly generated successfully transmitted packets and successfully retransmitted packets, and it is computed as [6]:

$$\overline{G} = (K - \overline{n}) P_o + \overline{n} P_r \tag{21}$$

where $\overline{n}$ is the expected channel backlog; P_o is the probability of the user to generate and transmit a new packet at the beginning of the next time slot; P_r is the probability of the backlogged packet retransmissions occur in any given time slot, and P_C is the success packet probability in the corresponding system given by $P_C = [1 - P_b]^L$, where P_b is the bit error rate (BER) and L is the packet length in bits. Assuming Gaussian noise approximation, the BER is related to its SINR by $P_b = 1/2\ \mathrm{erfc}(\sqrt{\gamma}/2)$, where erfc(·) is the complementary error function [4,5].

5. Results

In all numerical results, typical parameter values for the optical network devices and standard fiber were assumed. These parameters are summarized in Table 1 [2,23,26].

Note that the usual receiver noise power in (2) includes thermal noise, shot noise and optical preamplifier noise [3]. However, the amplified spontaneous emission (ASE) in the optical preamplifier will be the main limiting factor (in addition to the MAI), compared to thermal and shot noise at the receiver [4]. The receiver noise power is represented

Table 1
System parameters.

Variable	Value
a – Fiber loss coefficient	0.2 dB/km
d_{ij} – link length	[4: 100] km
h – Planck constant	6.63×10^{-34} J/Hz
f – Light frequency	193.1 THz
B_o – Optical bandwidth	30 GHz
n_{sp} – Spontaneous emission factor	2
δ – Excess loss ratio	0.2 dB
G_{amp} – EDFA gain	20 dB
2-D OCDMA CHPC codes	(4 × 101, 4, 1, 1)
a_c – En/decoder loss	6 dB
w – Code weight	4
T_C – Chip period	4 ps
γ^* – Target SNIR	20 dB
L – Packet length	500 bits
K – Number of nodes	31

by $\sigma_i^2 = n_{sp} hf (G_{amp} - 1) B_o$ [3]. Hence, for instance, applying typical parameters of Table 1 immediately we obtain $\sigma_i^2 = 15 \times 10^{-7}\ \mathrm{A}^2$.

The code parameters are code weight of 4 and code length of 101, thus the code is characterized by $(4 \times 101, 4, 1, 0)$. In the calculation of the total round trip delays it was considered that light propagates at approximately $v = 2 \cdot 10^5$ km/s within the fiber and the power control algorithm is updated every 5 ms [27]. For the purpose of computational simulations, the scenario considered in our study is represented in Fig. 3. The distances between Tx nodes, considering 31 nodes, and star coupler are shown in Fig. 4(a), while distances between Rx nodes and star coupler are presented in Fig. 4(b). The nodes are uniformly distributed over a ring area with an internal radius of 2 km and an external radius of 50 km; hence, the range of the total link length is in between [4; 100] km.

5.1. Delay effect over the power allocation and convergence of FM-DPCA

The effects of delay over FM-DPCA are investigated in Figs. 5 and 6, considering the same network topology presented in Fig. 4, for $\alpha = 0.2$ and $\alpha = 0.5$, respectively. Fig. 5(a) and 6(a) show the transmitted power per user for the number of iterations with no time-delay. On the other hand, Figs. 5(b) and 6(b) depict the transmitted power per user for the number of iterations with the time-delay effect over the FM-DPCA convergence.

One can see that increasing the number of iterations causes the convergence of the transmitted power per user obtained by FM-DPCA to the values calculated by the centralized control strategy, represented by horizontal dot

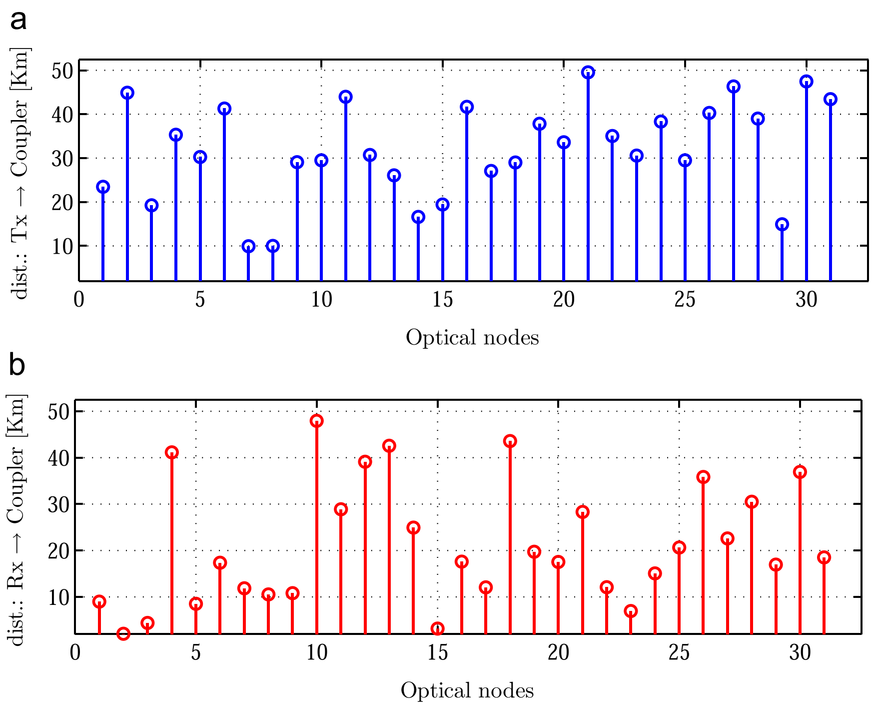

Fig. 4. (a) Distance between Tx nodes and star coupler. (b) Distance between Rx nodes and star coupler.

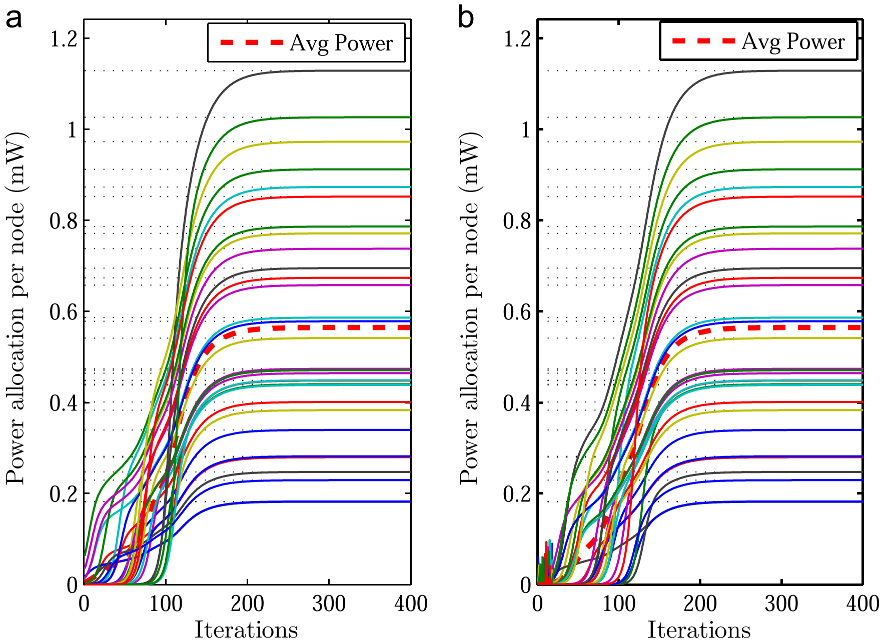

Fig. 5. Optimized power assignment per node versus the number of iterations for the distributed power control approach, considering 31 nodes and convergence factor $\alpha = 0.2$: (a) Without delay and (b) with delay.

lines. These numerical results for the optimized powers were obtained applying the centralized control strategy, i.e. solving (1) by matrix inversion. The drawback of centralized control strategy is the required awareness central node deploying information from the entire physical network architecture. Increasing the α value from 0.2 to 0.5 results in an increase of the mean convergence velocity by approximately 110 iterations; however, it is necessary to respect the limitation of maximum value of α bounded by (17). Note that when the delay is considered (Figs. 5(b) and 6(b)) there is a transient in the transmitted power per user for initial iterations. Furthermore, one can observe that when the delay effect is included, it is necessary more iteration for the FM-DPCA algorithm achieve full convergence for the transmitted power. Therefore, when Fig. 5(a) and (b) is compared, it is necessary a mean of approximately more 14 iterations to achieve the convergence. In addition, when Fig. 6(a) and (b) is compared, it is necessary a mean of approximately more 18 iterations to achieve the convergence. The difference between the numbers of needed iterations is related with the quality of the solutions from the FM-DPCA, which decreases with the increase of α [10].

Next, the effects of delay over the feedback closed-loop power assignment are investigated in Figs. 7 and 8 , considering the same scenario presented in Fig. 4 with the same convergence factor α of 0.2 and 0.5, respectively. Figs. 7(a) and 8(a) show the error function per user, given by (9), against the number of iterations without any delay. On other hand, Figs. 7(b) and 8(b) show the modulus of error function, given by (9), per user for the number of iterations with delay.

As expected, the increasing of the number of iterations results in the error reduction and this error became zero when the convergence of the SNIR obtained by FM-DPCA has reached the SNIR target value. From Figs. 7(a) and 8(a) it is necessary an average of ≈ 205 and ≈ 95 iterations to achieve the zero error, respectively. This difference is related with the convergence factor.

Furthermore, when the delay is considered (Figs. 7(b) and 8(b)), the FM-DPCA needs more iterations to achieve full convergence, i.e., zero-error. From Figs. 7(b) and 8(b) it is necessary an average of ≈ 219 and ≈ 113 iterations, respectively, for the FM-DPCA achieve the zero-error. It also can be seen that increasing the α value results in an increase of the convergence velocity; however, for higher α the error amplitude is larger to force convergence. One can observe this characteristic comparing curves of Fig. 7(a) and (b) with those of Fig. 8(a) and (b), where the variation between the mean amplitude of α from 0.2 to 0.5 is approximately 20% and 17.5% of the cases without delay (Figs. 7(a) and 8(a)) and with delay (Figs. 7(b) and 8(b)), respectively. This effect has been also observed in the FM-DPCA algorithm operating in wireless networks, where the SNIR convergence towards the objective value presents oscillatory behavior [15].

5.2. Uncertainty in the estimated SNIR and NMSE

Next, the uncertainty of the estimated and the real SNIR values is analysed considering its impact on the power allocation per node and the associated NMSE, as depicted in Figs. 9 and 10, respectively. Indeed, Fig. 9(a) and (b) shows the power allocation per node for the number of iterations considering a high level of uncertainty of 50% on the estimated and the real SNIR values for convergence factor of (a) $\alpha = 0.2$ and (b) $\alpha = 0.5$, respectively.

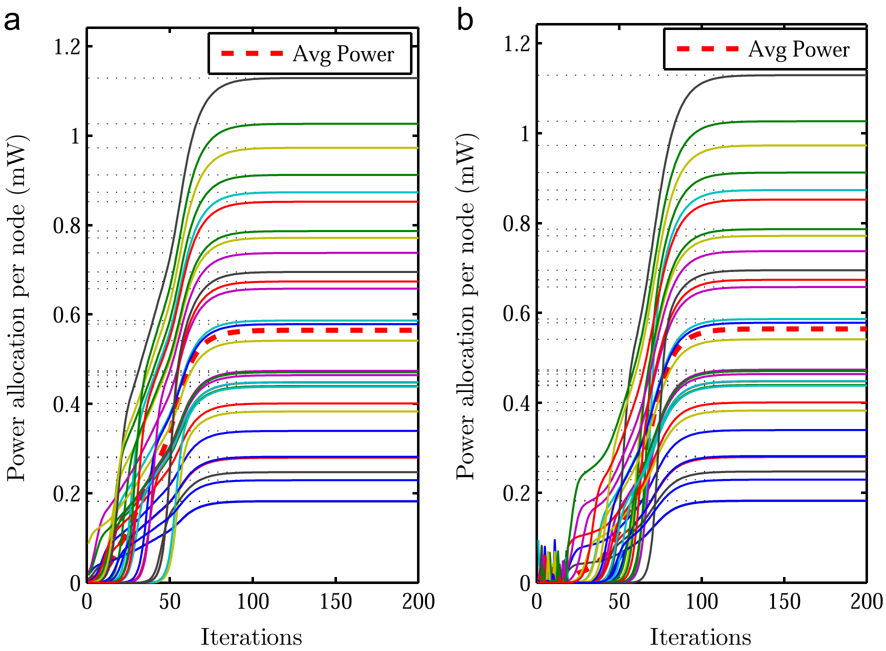

Fig. 6. Optimized power assignment per node versus the number of iterations for the distributed power control approach, considering 31 nodes and convergence factor $\alpha = 0.5$: (a) Without delay and (b) with delay.

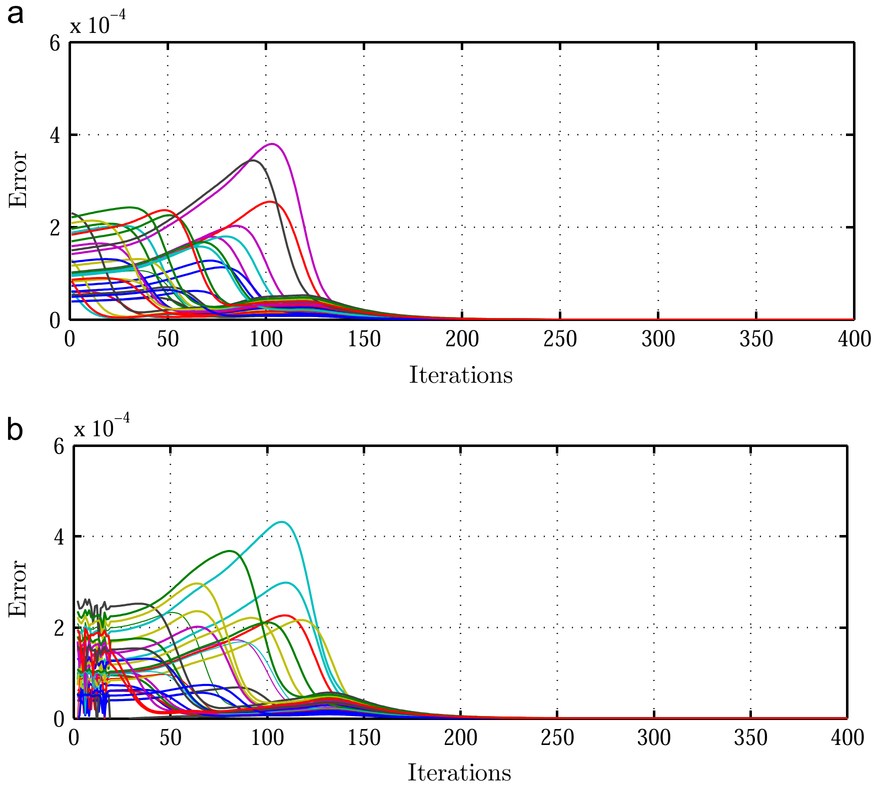

Fig. 7. Error per user versus the number of iterations for the distributed power control approach, considering 31 nodes and convergence factor $\alpha = 0.2$: (a) Without delay and (b) with delay.

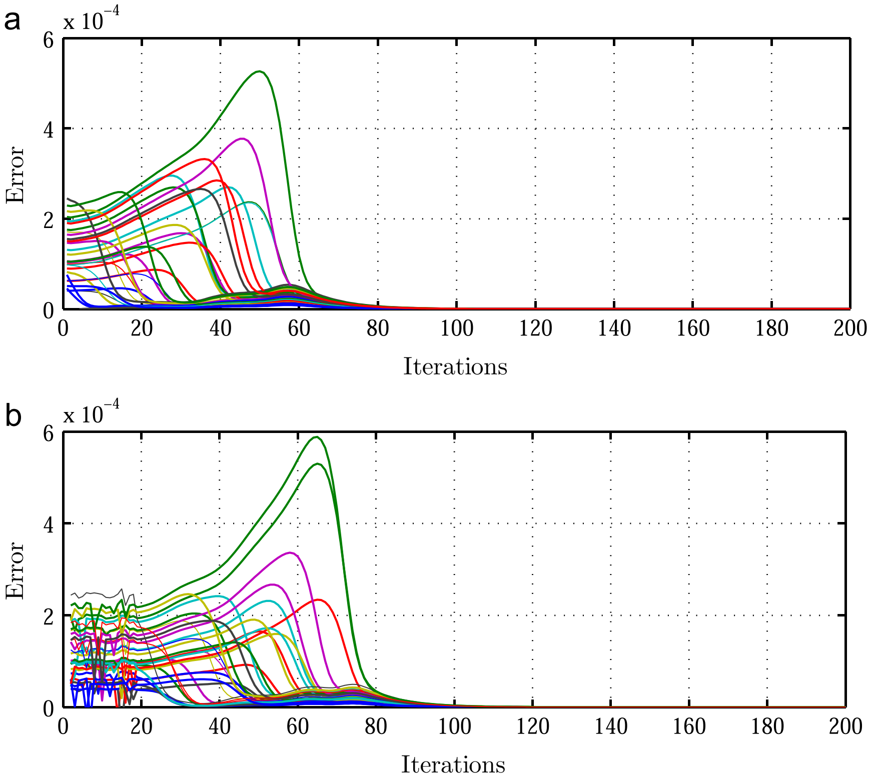

Fig. 8. Error per user versus the number of iterations for the distributed power control approach, considering 31 nodes and convergence factor $\alpha = 0.5$: (a) Without delay and (b) with delay.

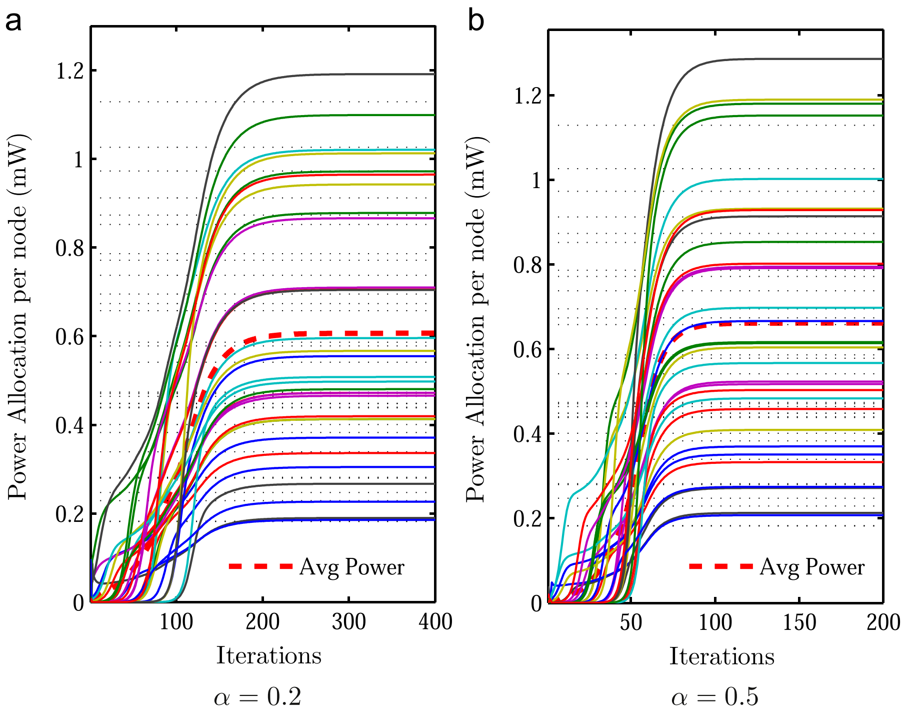

Fig. 9. Optimized power assignment per node versus the number of iterations for the FM-DPCA approach, considering 31 nodes and uncertainty of 50% of the estimated and the real SNIR value (a) $\alpha = 0.2$. (b) $\alpha = 0.5$.

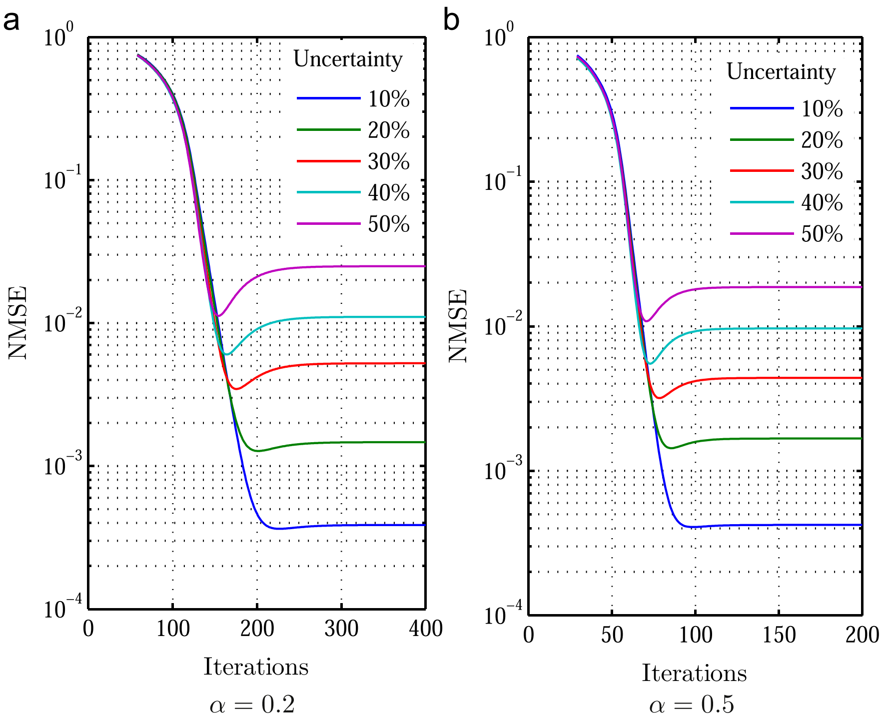

Fig. 10. NMSE versus the number of iterations for the FM-DPCA approach, considering 31 nodes and uncertainty in the range [10%;50] of the estimated and the real SNIR value (a) $\alpha = 0.2$. (b) $\alpha = 0.5$.

One can see the impact of the uncertainty on the estimated SNIR and as a consequence on the power allocation, that is observed by the difference among the transmitted power per user obtained by the FM-DPCA after full convergence to the values calculated by the centralized control strategy (horizontal dot lines values). Note that even the FM-DPCA approach presenting smaller discrepancy from the optimum power vector solution, the uncertainty on the distributed SNIR estimation definitively degrades the quality of power vector solution. As expected, increasing the convergence factor causes the increase of the convergence speed of the transmitted power per user, although the difference among the transmitted power values obtained by FM-DPCA after full convergence regarding the values obtained by the centralized control strategy does not present variation with the convergence factor value increment.

A quantitative analysis related the impact of the uncertainty in the estimated SNIR is obtained straightly by NMSE analysis. The NMSE evolution against the number of iteration is presented in Fig. 10 considering uncertainty of 10%, 20%, 30%, 40% and 50% of the estimated and the real SNIR value. As one can observe from Fig. 10, the NMSE is decreasing with the number of iterations and the NMSE decreases with the uncertainty of increasing in the SNIR estimation. Note that the oscillatory behaviour of the NMSE becomes more noticeable for higher level of uncertainty (40% and 50%) in the SNIR estimation. This behaviour results from the difficulty faced by the FM-DPCA to converge under high variation of the SNIR. On the other hand, the increasing of NMSE represents the decreasing of the quality of the solutions.

It is worth noting that FM-DPCA algorithm presents small power consumption per node when compared with the FM without delay and uncertainties [12]; however, the increase of NMSE implies the power consumption increasing. In this context, the convergence of the DPCA occurs with an extra power expense of transmitted power due to the uncertainty in the SNIR estimation.

5.3. Packet delay performance

The impact of the FM-DPCA procedure on the packet delay performance is analyzed hereby considering the same scenario illustrated in Fig. 4 for the packet length of $L = 500$ bits. Fig. 11 depicts the relation between the throughput and the packet delay for (a) $\alpha = 0.2$ and (b) $\alpha = 0.5$, considering three different configurations: (i) FM-DPCA without delay; (ii) FM-DPCA with delay and (iii) without FM-DPCA. The FM-DPCA algorithm is considered for the situations without the system delay and with the system delay for the total convergence of the algorithm. On the other hand, for the scenario without FM-DPCA, the transmitted power for each node was evaluated by a static power budget, i.e. without effects of MAI or taking into consideration the number of active nodes.

From Fig. 11 one can infer that the throughput and the average packet delay increase until the throughput reaches its saturation value. The throughput saturation occurs for both α value of at approximately 20 and 30 packets/slot for the cases (iii) without FM-DPCA and (i) without delay, respectively. This quantitative difference of almost 10 packets/slot justifies the needed of FM-DPCA procedure and its implementation in a OCDMA network. In fact,

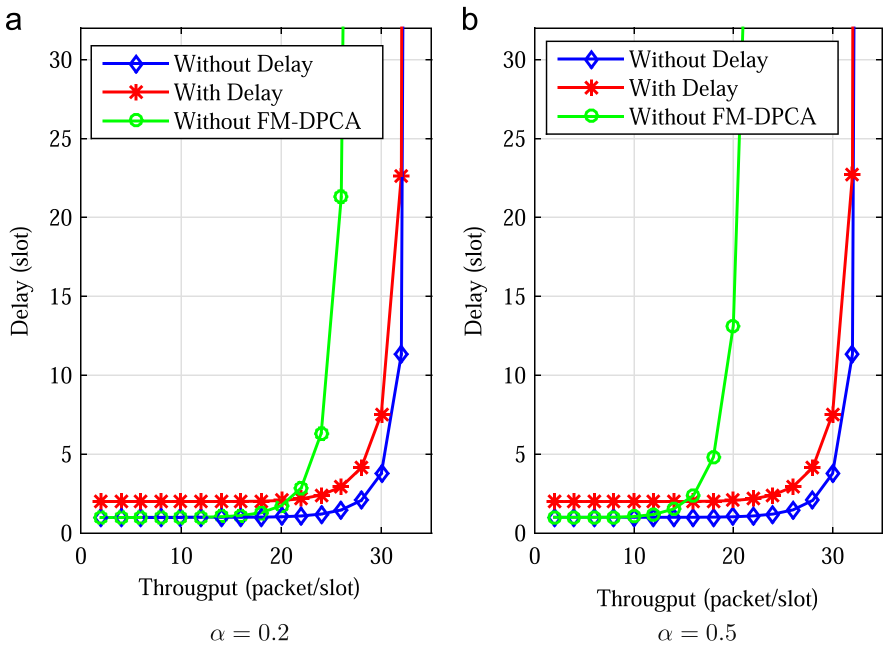

Fig. 11. Packet delay in terms of number of slots *versus* optical system throughput, considering three different configurations: FM-DPCA without delay, FM-DPCA with delay and without FM-DPCA. (a) $\alpha = 0.2$. (b) $\alpha = 0.5$.

without the power control provided by the FM-DPCA algorithm, the SINR declines and the packets become more vulnerable to distortion, which reduces the likelihood of their successful transmission and reception. Thus, the probabilities of correct packets collapse, and hence, the packet delay could substantially increase. On the other hand, the effects of the system delay could be observed by the increase of the packet delay of approximately 1 packet/slot when the configuration (i) with delay is compared with case (iii) without delay, both of them equipped with FM-DPCA algorithm. This packet delay occurs when the time slot increases to accommodate the overall system delay.

6. Conclusions

In this work the performance of a distributed power control algorithm (DPCA) based on the Foschini and Miljanic model (FM-DPCA) considering the time-delay and estimation uncertainty has been investigated. The delay that results from the processing time (coding and decoding), propagation delay and waiting for availability of channels for transmission is inevitably present in the communication subject to interference in realistic multiple access optical networks. Aspects of control theory have been deployed aiming to derive the FM algorithm model, as well as to obtain results with the objective to study the stability properties under time-varying delays and estimation uncertainty. The advantage of using a control theory framework is that stability and estimation uncertainty can be jointly analysed.

The numerical results have demonstrated the convergence of transmitted power vector obtained from FM-DPCA algorithm operating under delay introduction; however, a noticeable transient behaviour over the initial iterations introduces a time lag in the FM-DPCA algorithm convergence. Furthermore, when the system delay is introduced, there is the necessity of more iterations to the convergence, while increasing the value of convergence factor α results in the acceleration of the convergence at expense of error amplitude increment.

The impact of the uncertainty on the estimated SNIR, and as a consequence on the power allocation has been analysed; the FM-DPCA algorithm convergence has been verified even when high level of uncertainty is introduced. A quantitative analysis regarding the impact of the uncertainty on the estimated SNIR demonstrated the quality of the solutions decrease (in terms of NMSE), specially under high level of uncertainty.

Acknowledgments

This work was supported in part by the Araucaria Foundation, PR, Brazil, under Grant 668/2014, National Council for Scientific and Technological Development (CNPq) of Brazil under Grant 304358/2012-6, 446995/2014-2 and State University of Londrina-Paraná State Government (UEL).

References

[1] E. Wong, Next-generation broadband access networks and technologies, J. Lightwave Technol. 30 (4) (2012) 597–608.
[2] H. Yin, D. Richardson, Optical Code Division Multiple Access Communication Networks: Theory and Applications, Springer-Verlag and Tsinghua University Press, Berlin, 2009.

[3] N.G. Tarhuni, T.O. Korhonen, M.S. Elmusrati, E. Mutafungwa, Power control of optical cdma star networks, Opt. Commun. 259 (1–3) (2006) 655–664.

[4] F.R. Durand, M.S. Filho, T. Abrão, The effects of power control on the optical CDMA random access protocol, Opt. Switch. Netw. 9 (1) (2012) 52–60.

[5] S. Khaleghi, M.-R. Pakravan, Quality of service provisioning in optical cdma packet networks, IEEE/OSA J. Opt. Commun. Netw. 2 (5) (2010) 283–292.

[6] R. Raad, E. Inaty, P. Fortier, H.M.H. Shalaby, Optimal resource allocation scheme in a multirate overlapped optical cdma system, J. Lightwave Technol. 25 (8) (2007) 2044–2053.

[7] M. Tang, C. Long, X. Guan, Nonconvex optimization for power control in wireless cdma networks, Wirel. Pers. Commun. 58 (4) (2011) 851–865.

[8] L. Pavel, Game Theory for Control of Optical Networks, Springer-Birkhauser, New York, USA, 2012.

[9] F.R. Durand, L. Melo, L.R. Garcia, A.J. dos Santos, T. Abrão, Optical network optimization based on particle swarm, in: T. Abrão (Ed.), search Algorithms for Engineering Optimization, Intech, 2013, part 6, pp. 143–172.

[10] G. Foschini, Z. Miljanic, A simple distributed autonomous power control algorithm and its convergence, IEEE Trans. Veh. Technol. 42 (4) (1993) 641–646.

[11] P.F. Verhulst, Notice sur la loi que la population pursuit dans son accroissement, Corresp. mathématique phys. 10 (1838) 113–121.

[12] T.J. Gross, T. Abrão, P.J.E. Jeszensky, Distributed power control algorithm for multiple access systems based on verhulst model, AEU – Int. J. Electron. Commun. 65 (4) (2011) 361–372.

[13] D.U. Campos-Delgado, M. Luna-Rivera, Unified framework for the analysis and design of linear uplink power control in cdma systems, Wirel. Netw. 18 (4) (2012) 427–441.

[14] J. Baillieul, P. Antsaklis, Control and communication challenges in networked real-time systems, Proc. IEEE 95 (1) (2007) 9–28.

[15] D. Campos Delgado, J. Luna Rivera, Performance study of distributed power control algorithms under time-delays and measurement uncertainty, IEEE Latin Am. Trans. (Revista IEEE America Latina) 11 (2) (2013) 690–697.

[16] D.U. Campos-Delgado, J.M. Luna-Rivera, F.J. Martnez-Lopez, Distributed power control algorithms in the uplink of wireless code-division multiple-access systems, IET Control Theory Appl. 4 (5) (2010) 795–805.

[17] T. Charalambous, I. Lestas, G. Vinnicombe, On the stability of the Foschini–Miljanic algorithm with time-delays, in: the 47th IEEE Conference on Decision and Control (CDC), 2008, pp. 2991–2996.

[18] T. Charalambous, Y. Ariba, On the stability of a power control algorithm for wireless networks in the presence of time-varying delays, in: the 10th European Control Conference (ECC), 2009.

[19] F. Tadeo, A. Hmamed, A. Benzaouia, T. Alvarez, Properties of power control algorithms in wireless networks with delays: a positive systems approach, in: UKACC International Conference on Control 2010, 2010, pp. 1–6.

[20] I. Lestas, Power control in wireless networks: stability and delay independence for a general class of distributed algorithms, IEEE Trans. Autom. Control 57 (5) (2012) 1253–1258.

[21] A. Zappavigna, T. Charalambous, F. Knorn, Unconditional stability of the Foschini–Miljanic algorithm, Automatica 48 (1) (2012) 219–224.

[22] B. Birand, H. Wang, K. Bergman, D. Kilper, T. Nandagopal, G. Zussman, Real-time power control for dynamic optical networks – algorithms and experimentation, in: 21st IEEE International Conference on Network Protocols (ICNP), 2013, pp. 1–10.

[23] C.-S. Brès, P. Prucnal, Code-empowered lightwave networks, J. Lightw. Technol. 25 (10) (2007) 2911–2921.

[24] L.D.H. Sampaio, T. Abrão, B.A. Angélico, M. Fernando Lima, M. L. Proença Jr., P.J.E. Jeszensky, Hybrid heuristic-waterfilling game theory approach in MC-CDMA resource allocation, Appl. Soft Comput. 12 (7) (2012) 1902–1912.

[25] G.H. Golub, C.F. Van Loan, Matrix Computations, 3rd ed., Johns Hopkins University Press, Baltimore, MD, USA, 1996.

[26] Y.-K. Huang, V. Baby, I. Glesk, C.-S. Bres, C. Greiner, D. Iazikov, T. Mossberg, P. Prucnal, Novel multicode-processing platform for wavelength-hopping time-spreading optical CDMA: a path to device miniaturization and enhanced network functionality, IEEE J. Sel. Top. Quantum Electron. 13 (5) (2007) 1471–1479.

[27] Y. Pan, T. Alpcan, L. Pavel, A system performance approach to osnr optimization in optical networks, IEEE Trans. Commun. 58 (4) (2010) 1193–1200.